Upper-Ocean Thermal Variations in the North Pacific during 1970–1991

CLARA DESER, MICHAEL A. ALEXANDER, AND MICHAEL S. TIMLIN

CIRES, University of Colorado, Boulder, Colorado

(Manuscript received 7 March 1995, in final form 22 January 1996)

ABSTRACT

A newly available, extensive compilation of upper-ocean temperature profiles was used to study the vertical structure of thermal anomalies between the surface and 400-m depth in the North Pacific during 1970–1991. A prominent decade-long perturbation in climate occurred during this time period: surface waters cooled by ~1°C in the central and western North Pacific and warmed by about the same amount along the west coast of North America from late 1976 to 1988. Comparison with data from COADS suggests that the relatively sparse sampling of the subsurface data is adequate for describing the climate anomaly.

The vertical structure of seasonal thermal anomalies in the central North Pacific shows a series of cold pulses beginning in the fall of 1976 and continuing until late 1988 that appear to originate at the surface and descend with time into the main thermocline to at least 400-m depth. Individual cold events descend rapidly (~100 m yr^{-1}), superimposed upon a slower cooling (~15 m yr^{-1}). The interdecadal climate change, while evident at the surface, is most prominent below ~150 m where interannual variations are small. Unlike the central North Pacific, the temperature changes along the west coast of North America appear to be confined to approximately the upper 200–250 m. The structure of the interdecadal thermal variations in the eastern and central North Pacific appears to be consistent with the dynamics of the ventilated thermocline. In the western North Pacific, strong cooling is observed along the axis of the Kuroshio Current Extension below ~200 m depth during the 1980s.

Changes in mixed layer depth accompany the SST variations, but their spatial distribution is not identical to the pattern of SST change. In particular, the decade-long cool period in the central North Pacific was accompanied by a ~20 m deepening of the mixed layer in winter, but no significant changes in mixed layer depth were found along the west coast of North America. It is suggested that other factors such as stratification beneath the mixed layer and synoptic wind forcing may play a role in determining the distribution of mixed layer depth anomalies.

1. Introduction

Because of their large thermal inertia, the oceans are expected to play a major role in driving climate variations on timescales of decades and longer. One well-documented example of recent climate change is the decade-long shift that began in late 1976 over the North Pacific (cf. Douglas et al. 1982; Nitta and Yamada 1989; Trenberth 1990; Trenberth and Hurrell 1994; Graham 1994). From approximately 1977 to 1988, particularly during the winter-half of the year, the atmospheric circulation over the North Pacific was characterized by a deeper than normal Aleutian low pressure system, accompanied by stronger than normal westerly winds across the central North Pacific and enhanced southerly flow along the west coast of North America (Fig. 1). Sea surface temperatures (SSTs) during this time period were below normal in the central North Pacific and above normal along the California coast northward to the Gulf of Alaska. The climate change also affected marine biological activity, including phytoplankton biomass in the central and North Pacific (Venrick et al. 1987; Polovina et al. 1995) and salmon catch in Alaska (Ebbesmeyer et al. 1991; Beamish and Bouillon 1993).

The cause of the climate anomaly is still a matter of debate. Some studies suggest that the relative warmth of the tropical Pacific since 1976 may have contributed to the deepening of the Aleutian low via Rossby wave dynamics and the accompanying reorganization of the midlatitude stormtrack transients (cf. Trenberth 1990; Chen et al. 1992; Graham et al. 1994; Kumar et al. 1994). An alternative view has been put forth by Latif and Barnett (1994), who suggest that a coupled instability of the midlatitude ocean–atmosphere system can give rise to decadal climate variations. Regardless of the cause of the atmospheric circulation change, the hypothesis that the decade-long SST shift in the North Pacific was forced by the atmosphere has been tested in an ocean general circulation modeling experiment by Miller et al. (1994) and Cayan et al. (1995). Using prescribed surface boundary conditions taken from observations, Miller et al. (1994) and Cayan et al. (1995) realistically simulated the SST changes in the North Pacific. In the model, SSTs over the central North Pacific cooled via anomalous surface heat fluxes, entrainment, and advection by Ekman currents, while SSTs

Corresponding author address: Dr. Clara Deser, CIRES, Campus Box 449, University of Colorado, Boulder, CO 80309.
E-mail: cxd@cdc.noaa.gov

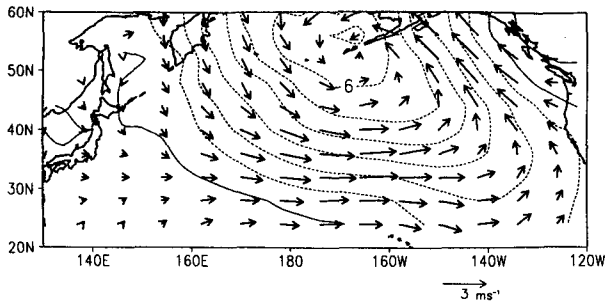

FIG. 1. Winter (Nov–Mar) surface wind (arrows) and sea level pressure (contours) differences between 1977–88 and 1971–76. Contour interval is 1 mb; negative contours are dashed.

along the California coast warmed primarily by anomalous surface heat fluxes. Changes in mixed layer depth were found to accompany the model SST variations.

While the atmospheric and surface oceanic aspects of the decade-long Pacific climate anomaly are well documented, little is known about the changes beneath the ocean surface. Talley and White (1987) noted a cooling trend at 300 m in the central North Pacific from 1976 to 1984, while Antonov (1993) showed that the cooling of the North Pacific as a whole during 1957–1981 was confined to above 500–600 m. A more complete description of the observed vertical structure of the oceanic thermal changes may shed light on the mechanisms that produced the climate change, as well as provide important verification for ocean modeling experiments. For example, is the scenario of Miller et al. (1994) consistent with the observed vertical structure (e.g., can one see thermal anomalies propagate downward from the ocean surface)? How deep do the thermal anomalies penetrate? Are they confined to the upper mixed layer, or do they extend into the permanent thermocline? Does the Kuroshio Current System exhibit any changes? Does the mixed layer in the central (eastern) North Pacific deepen (shoal) as modeled by Miller et al. (1994)?

The purpose of this study is to document the observed vertical structure of the thermal changes in the upper 400 m of the North Pacific Ocean during 1970–1991. We use the recently expanded compilation of upper-ocean temperature profiles from Levitus and Boyer (1994). The dataset and processing techniques are described in section 2. The vertical structure of the subsurface thermal changes is documented in section 3. We discuss the results in section 4 and summarize our findings in section 5.

2. Data

The subsurface ocean temperature profiles used in this study are from the *World Ocean Atlas 1994* (WOA94) of Levitus and Boyer (1994). These data were recovered as part of a recent and extensive search through international archives and then quality controlled in a consistent manner (Boyer and Levitus 1994). While subsurface temperature data have been collected for more than 50 years, data coverage became sufficient to study basinwide patterns in the North Pacific in the early 1970s. Here we examine the temperature field in the upper 400 m of the North Pacific from 1970 to 1991 using three types of instruments: expendable bathythermographs (XBTs), mechanical bathythermographs (MBTs), and station data (SD), primarily from Nansen bottles.

Figure 2a shows the total number of observations summed over the North Pacific (50°–22°N, 140°E–120°W) as a function of time for the three instrument types. In the early 1970s, there are approximately 200–800 profiles per month from each instrument type. After 1975, the majority of observations are from XBTs ($500 \sim 1500$ mo^{-1}). Figure 2b shows the spatial distribution of all three data types combined, expressed as the percent of months with data during 1970–1991. The temporal coverage exceeds 90% in the eastern North Pacific and off Japan and exceeds 70% along the

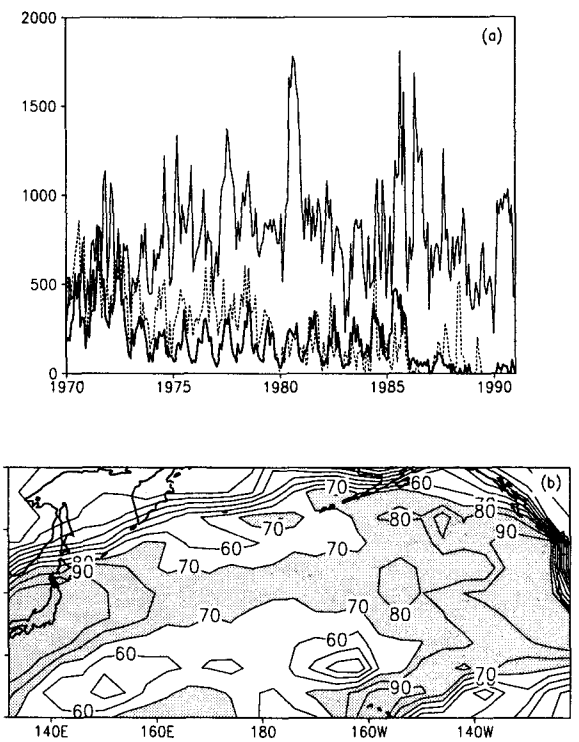

FIG. 2. (a) Total number of upper-ocean temperature profiles in the North Pacific (50°–22°N, 140°E–120°W) per month by instrument type: Station data (SD; thick solid curve), expendable bathythermographs (XBT; thin solid curve), and mechanical bathythermographs (MBT; thin dashed curve). (b) Percent of months during 1970–91 containing at least one upper-ocean temperature profile per 4° × 4° grid box. Values greater than 70% are shaded; contour interval is 10%.

shipping lanes between Japan and North America and between Hawaii and the United States.

In the WOA94, the temperature profiles are interpolated to standard levels (0 m, 10 m, 20 m, 30 m, 50 m, 75 m, 100 m, 125 m, 150 m, 200 m, 250 m, 300 m, 400 m) using the criterion that the maximum distance from the standard level to observed adjacent shallower and deeper levels is 50 m for depths above and including 200 m and 100 m for depths between 250 m and 800 m (Boyer and Levitus 1994). Since most XBTs record data at inflection points (e.g., where the slope of the temperature profile changes), they do not contain reports within the mixed layer. Thus, when the mixed layer is deep (e.g., in winter), the depth criteria used for interpolation results in missing values at standard levels within the mixed layer. To retrieve temperatures at standard levels within the mixed layer from the XBT data, we linearly interpolated the inflection point data to standard levels without any depth criteria, excluding data which were flagged as erroneous. For the North Pacific as a whole, more than 40% of the temperature data in the WOA94 are missing at standard levels within the winter mixed layer (above ~100 m), but less than 5% are missing after our interpolation scheme is applied (see Timlin et al. 1995).

We formed monthly anomalies on a 1° × 1° grid at each standard level from the surface to 400 m as departures from the Levitus and Boyer (1994) monthly 1° × 1° climatology, and then spatially averaged the 1° × 1° anomalies into 4° × 4° grid boxes. The Levitus and Boyer climatology is based on an objective analysis of all available temperature data since 1900. The choice of 400 m as a lower limit for our analysis reflects that the majority of XBTs sample down to ~450 m (Levitus and Boyer 1994). We have repeated all of the analyses shown in this study using XBT observations only and find no significant differences with the results based on the combined data types.

Because the WOA94 subsurface dataset is relatively new, we address briefly the question of data quality by comparing the surface observations with SSTs from the Comprehensive Ocean–Atmosphere Data Set (COADS) in section 3. The COADS has been used extensively for climate studies and contains an order of magnitude more surface observations than the WOA94 dataset over the North Pacific.

We computed a mixed layer depth (MLD) from each individual profile using linear interpolation between observed levels to find the first depth at which the temperature was 0.5°C lower than the SST (profiles with temperature inversions of more than 0.5°C were omitted). Different temperature criteria for MLD, such as 0.3°C or 1°C, gave qualitatively similar results. Note that this definition of MLD, also used by Levitus (1982) and Yan and Okubo (1992), excludes the contribution of salinity to the density stratification. Salinity may be expected to play an important role in the subpolar gyre (north of ~42°N), where temperatures are low, but only a minor role in the subtropical gyre (W. Large 1995, personal communication). We then formed monthly medians of the individual MLDs in each 4° × 4° grid box. Monthly MLD anomalies were defined as the departures from the long-term monthly medians, where 10 years were required to form the long-term median.

3. Results

As background to the analysis of thermal changes during 1970–1991, it is helpful to consider the long term mean distributions of temperature and mixed layer depth (MLD). Figure 3 shows the annual mean temperature climatology at depths 0 m, 250 m, and 400 m. At the surface, the isotherms are nearly zonal except for a slight tilt near the west coast of North America. The gyre circulations are prominent at 250- and 400-m depth: the anticyclonic flow around the subtropical gyre (20° ~ 40°N) is evidenced by the southward curv-

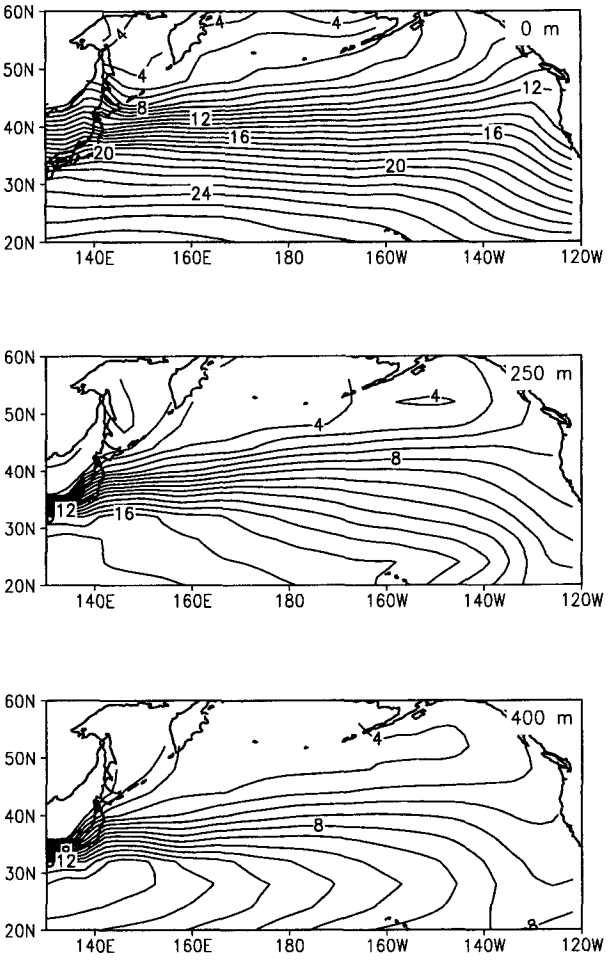

FIG. 3. Climatological distributions of annual mean temperature at depths 0 m, 250 m, and 400 m from the data of Levitus and Boyer (1994). Contour interval is 1°C in each panel.

ing of the isotherms in the eastern portion of the basin and the cyclonic flow around the subpolar gyre (40° ~ 60°N) by the northward bending of the isotherms in the Gulf of Alaska. The strongest meridional temperature gradients at 250 and 400 m are located between 33°N and 40°N west of ~170°E, marking the axis of the Kuroshio Current Extension. At the surface, the maximum meridional gradients are between 35° and 45°N, several degrees north of those at 400 m.

The climatological distributions of MLD in winter (Jan–Mar) and summer (Jul–Sep) are shown in Fig. 4. Summer MLDs are approximately 20–30 m over most of the North Pacific, while winter MLDs range from ~80 m along the west coast of the United States and south of ~25°S to ~160 m off the southern coast of Japan and >180 m in the central Pacific north of ~42°N. Winter MLDs in the subpolar gyre were not computed due to temperature inversions in a large number of the profiles. The MLD distributions are largely consistent with those of Levitus (1982) for the subtropical gyre. The deep winter mixed layers in the far western Pacific are confirmed by Suga and Hanawa (1990), who documented mixed layers as deep as 300–400 m in individual winters. They note that this area is a formation region for subtropical mode water.

To define the dominant pattern of SST variability during the period of subsurface observations, we computed empirical orthogonal functions of annual SST anomalies from the COADS during 1970–1991. The annual SST anomalies are January–December averages of the individual monthly departures from the monthly long-term means. The EOF is based on the covariance matrix, but similar results are obtained for the correlation matrix. Figure 5a shows the leading EOF in correlation form (e.g., the time series of the EOF was correlated with the original data). The EOF, which explains 34% of the variance, exhibits anomalies of one sign in the central North Pacific extending into the western Pacific along 40°N and anomalies of the opposite sign along the coast of North America. The correlation coefficients exceed 0.8 in absolute value near 35°N, 160°W and along the coast. Many other studies have shown similar EOF patterns, including Weare et al. (1976) and Namias et al. (1988). The time series of the expansion coefficient of the EOF, shown in Fig. 5b, exhibits a low-frequency component, with positive values during 1970–76, negative values during 1977–88, and a return to positive values during 1989–91. A similar EOF is found for surface temperatures from the WOA94 dataset (not shown).

We have investigated the seasonal dependence of the leading EOF of North Pacific SSTs. The first EOFs in autumn, winter, and spring are all very similar to that based on annual averages; in summer, the second EOF resembles the first EOF of the other seasons (not shown). As noted in the introduction, the interdecadal climate shift was also most pronounced in the atmosphere during the cool season (cf. Trenberth and Hurrell 1994).

On the basis of the EOF results, we computed SST differences between 1977–88 and 1970–76 using data

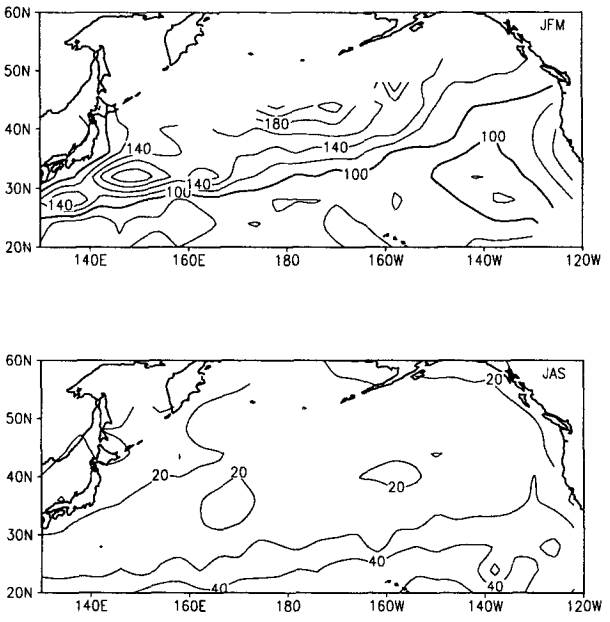

FIG. 4. Climatological distributions of mixed layer depth in winter (Jan–Mar; top) and summer (Jul–Sep; bottom). Contour interval is 20 m in winter and 10 m in summer.

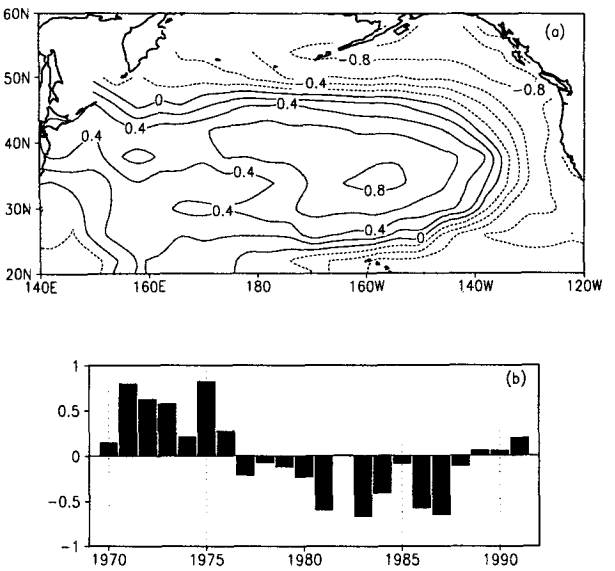

FIG. 5. (a) EOF 1 of annual SST anomalies over the North Pacific during 1970–91 from COADS. Contours denote correlation coefficients between the time series of the expansion coefficient of the EOF and the original data. Contour interval is 0.2. The EOF explains 34% of the variance. (b) Time series of the expansion coefficient of EOF 1. Units are relative.

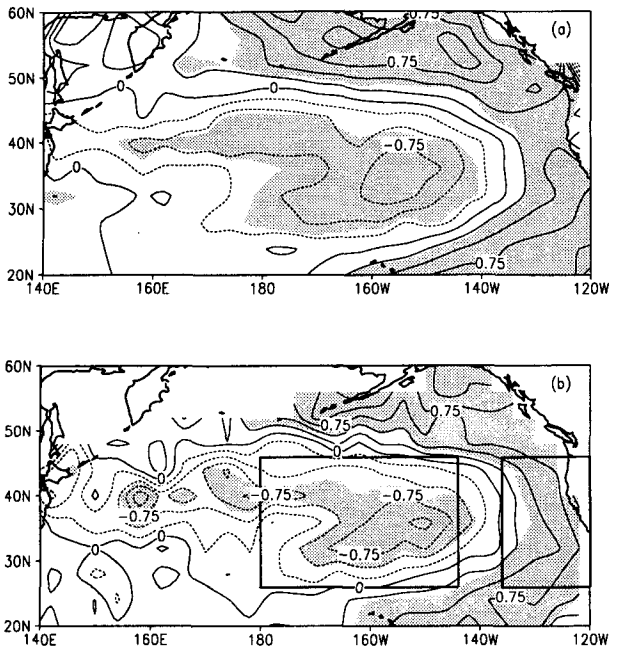

FIG. 6. Annual SST differences between 1977–88 and 1970–76 from (a) COADS and (b) WOA94. Contour interval is 0.25°C. Shading denotes SST differences that are significant at the 95% level. Rectangles in (b) show locations of the central and eastern North Pacific regions defined in the text.

from COADS (Fig. 6a) and WOA94 (Fig. 6b). The differences were computed from annual averages of the monthly anomalies, with a minimum of 3 months per year to define the annual average and 3 years to define the period average (1970–76 or 1977–88). No spatial smoothing has been applied to the results shown in Fig. 6. SST differences that are statistically significant at the 95% level according to a one-tailed Student's t-test are indicated by shading. The SST difference maps resemble the EOF, and are similar in both pattern and magnitude for the two datasets except in the far western Pacific where the cooling is stronger and exhibits considerable grid-scale variability in the WOA94 data. Maximum SST differences are ~0.75°C. The regions of maximum warming, and cooling east of ~165°E, are statistically significant at the 95% level in both datasets. The similarity of the SST differences in the COADS and WOA94 datasets suggests that the relatively sparse sampling of the WOA94 data is still adequate for capturing the interdecadal temperature change, except perhaps in the far western North Pacific (where, we note, synoptic variability associated with the Kuroshio Current Extension is large; cf. Levitus 1982). Nitta and Yamada (1989) and Trenberth and Hurrell (1994) show SST difference maps similar to Fig. 6.

Before examining the vertical structure of the interdecadal temperature change, it is necessary to know whether there is any time delay between the temperature anomalies at the surface and those at depth. For this purpose, we examined the vertical structure of the temperature anomalies in two key regions where the SST anomalies in Fig. 6 are large, statistically significant, and consistent between the two datasets, and where the data coverage is high: the central North Pacific (44°–28°N, 178°–146°W) and eastern North Pacific (44°–28°N, 134°–122°W). These regions are shown as rectangles in Fig. 6b. We note that limiting the northern boundary of either region to 40°N does not change the character of the results. While the Gulf of Alaska also merits study, the data volume in that region was not sufficient for our purposes.

a. The central Pacific region

The time–depth structure of the total and anomalous temperatures in the Central Region are shown in Figs. 7a and 7b. The anomalies are seasonal (Jan–Mar, Apr–Jun, Jul–Sep, Oct–Dec) averages of the monthly anomalies, with a minimum of 50% of the 4° × 4° grid boxes in the region contributing data in each season. The total temperatures were reconstructed from the sum of the area-averaged seasonal anomalies and area-averaged seasonal long-term means. The seasonal values have been smoothed with a three-point binomial filter.

The total temperature field (Fig. 7a) exhibits a permanent thermocline below ~125 m and a seasonal thermocline between ~25 m and ~75 m in summer (these depths were estimated from the long-term mean seasonal profiles). The surface cooling that began after 1976 is manifest as upward excursions of the 15°C isotherm in winter. Cooling is also found at depths within the permanent thermocline, where the isotherms rose approximately 30–50 m during the late 1970s and early 1980s.

The anomalous temperature field (Fig. 7b) shows a series of cold pulses beginning in the fall of 1976 that appear to originate at the surface during the cold season and move down through the water column. These episodic coolings become progressively more intense, penetrating deeper with time as evidenced by the downward migration of the −0.4°C contour. After 1982, the −0.4°C isotherm anomaly penetrates into the permanent thermocline. Although individual cold pulses descend relatively rapidly (~100 m yr^{-1}), the "envelope" of these cold pulses descends much more slowly (~15 m yr^{-1}).

Each of the cold pulses corresponds to a period of enhanced westerly winds, as shown in the bar graph directly above Fig. 7b. [The wind anomalies were obtained from COADS; note that in this region, a change in the zonal wind component corresponds to a change in wind strength (see Fig. 1).] We note that stronger westerlies can cool the mixed layer by increasing the loss of sensible and latent heat from the ocean surface, enhancing the rate of entrainment of cooler water at the base of the mixed layer, and increasing the southward

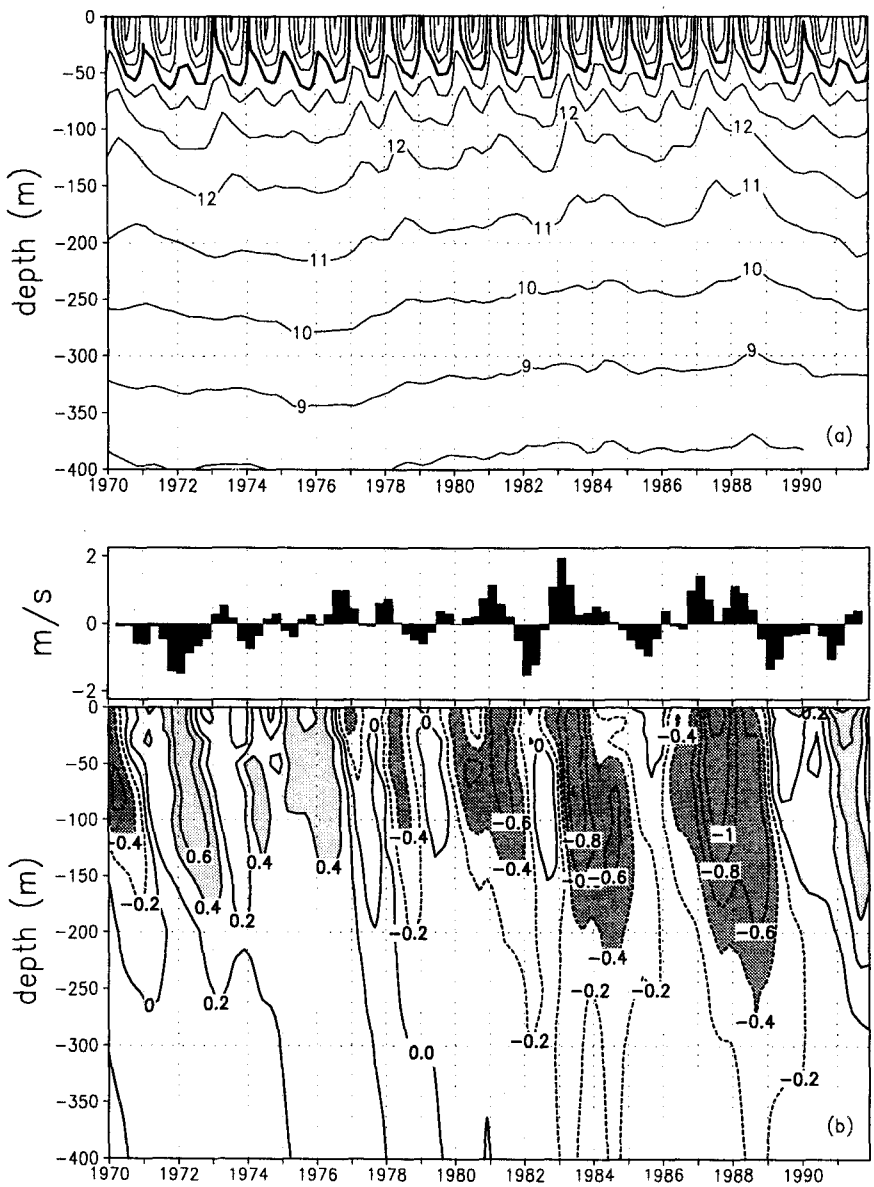

FIG. 7. Time–depth plot of seasonal (a) total and (b) anomalous temperature in the central North Pacific region. In (a), the contour interval is 1°C and the 15°C contour is thickened. In (b), the contour interval is 0.2°C, negative anomalies are dashed, and anomalies greater than 0.4°C (less than −0.4°C) are indicated by light (dark) shading. The 0°C contours are thickened. The bar graph directly above (b) shows seasonal zonal wind anomalies; positive (negative) values denote stronger (weaker) than normal winds from the west.

advection of cold water by Ekman currents (as shown also by Miller et al. 1994).

Another view of the thermal anomalies in the Central Region is given in Fig. 8, which shows seasonal temperature anomalies at selected depths. Note that the temperature scale changes with depth. While interannual variations are prominent in the mixed layer (0–100 m), the interdecadal change is clearest within the permanent thermocline (200–400 m). The progressive delay in the onset of cooling with depth is visually apparent (e.g., note the time of the first zero-crossing after 1976 at each depth).

To quantify the time delay with depth, we computed lag correlations between the temperature anomalies near the base of the winter mixed layer (100–150 m) in January–March and those at depth in each season (e.g., the time series of the winter anomalies at 100–150 m was correlated with the time series of the anom-

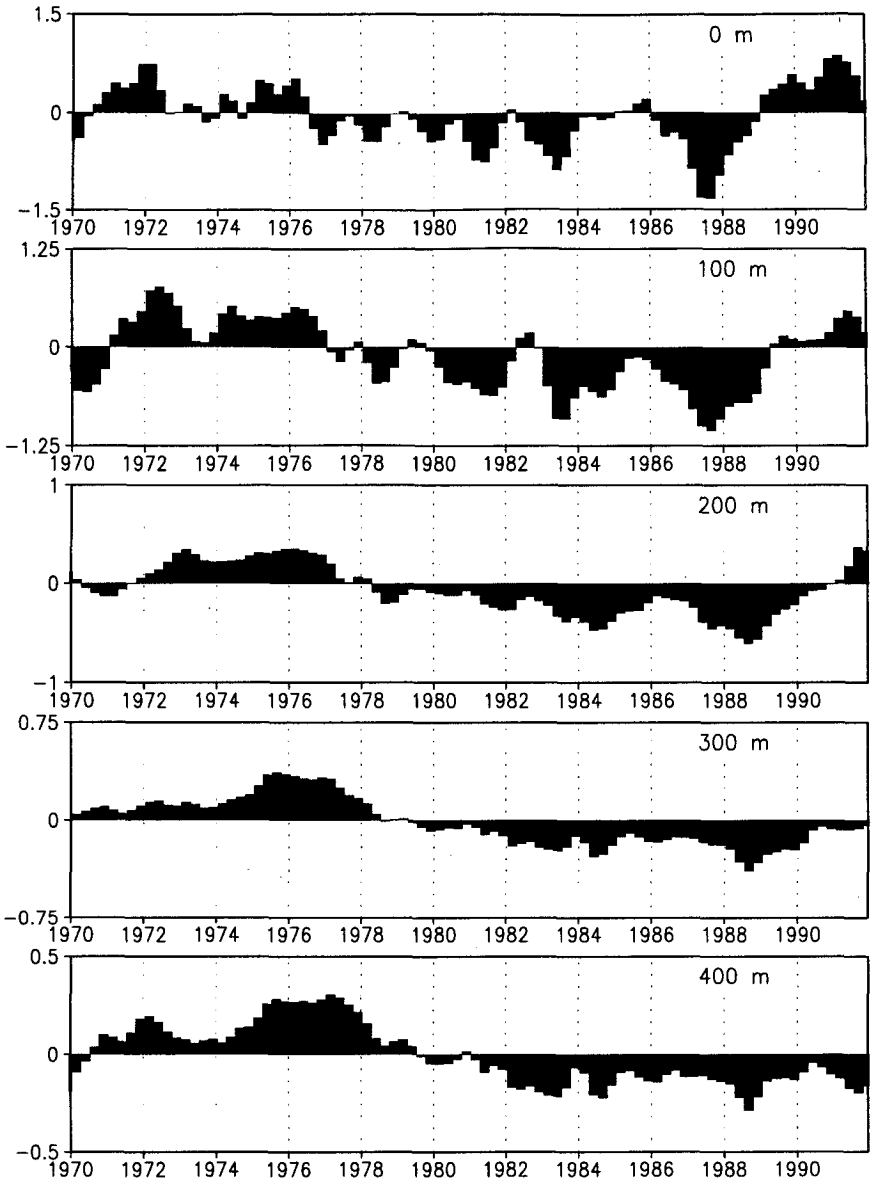

FIG. 8. Seasonal temperature anomalies (°C) in the central North Pacific region at selected depths. Note that the scale for the temperature anomalies is different for each depth.

alies in each season at each standard level). The correlations were then smoothed with a three-point running mean in time. The lag-correlation plot, shown in Fig. 9, confirms our visual impression that the winter mixed layer temperature anomalies descend at a rate of ~ 100 m yr^{-1} in the upper portion of the main thermocline (depth 150–400 m). It should be noted that Fig. 9 emphasizes the timescale of individual cold pulses and not the timescale associated with the "envelope" of the cold pulses, which is nearly an order of magnitude slower.

We examine the "slow" component of cooling in the central Pacific region further in Fig. 10, which shows the temperature anomalies for three consecutive 5-yr periods (1977–81, 1982–86, and 1987–91) as a function of depth and latitude for the longitude band 170°–145°W. These pentads were chosen to span the duration of the interdecadal cooling in the central Pacific region (recall Fig. 7b). In the early stage of cooling (Fig. 10a), the largest negative temperature anomalies (less than −0.3°C) are found in the upper 150 m between 30°N and 40°N. These anomalies move southward and downward over the next 10 years, becoming detached from the surface by the last pentad (Figs. 10b and 10c). We note that using low-pass filtered data in place of pentad aver-

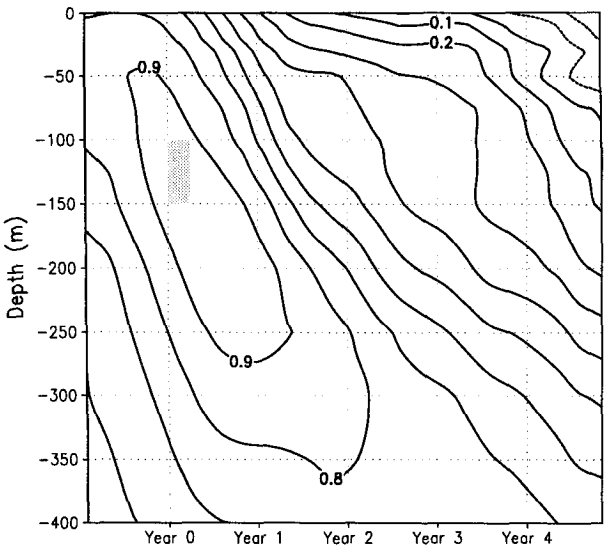

FIG. 9. Lag-correlations between temperature anomalies near the base of the mixed layer (100–150 m) in winter and seasonal temperature anomalies at depth in the central North Pacific region. Contour interval is 0.1.

ages yields a similar picture (not shown). We shall return to Fig. 10 in section 4.

b. *The eastern Pacific region*

Figure 11 shows the total and anomalous thermal structure for the eastern region. Like the central region, the warming in the eastern region proceeds in a series of discrete episodes (Fig. 11b). Some of these appear to originate at the surface (i.e., in 1977, 1978, 1980, and 1981), while others are centered at approximately 50–150 m depth (1984 and 1987) in the upper part of the main thermocline. These latter events may be associated with anomalous advection in the California Current System following tropical Pacific El Niño–Southern Oscillation (ENSO) activity (Enfield and Allen 1983; Simpson 1983; Rienecker and Mooers 1986; Pares Sierra and O'Brien 1989). Other warm episodes in the eastern region occur independently of ENSO, for example, those in 1980 and 1981. It may be noted that many of the cold and warm episodes in the eastern region correspond to events of the opposite sign in the Central Region, consistent with the EOF results.

In contrast to the central region, the thermal anomalies in the eastern region are primarily confined to the upper 200–250 m. The shallowness of the temperature anomalies in the eastern region may be in part a consequence of the strong mean vertical stratification in the upper part of the main thermocline that inhibits downward penetration of the mixed layer anomalies (see Fig. 11a). The mean stratification (as computed from salinity and temperature) between 100 and 200 m is approximately twice as strong in the eastern region as in the central region (not shown, but compare Figs. 7a and 11a). Other dynamical reasons for the shallowness of the interdecadal warming in the eastern region are discussed in section 4.

c. *Vertical structure of the interdecadal temperature change*

Having established the time delay of the thermal anomalies with depth in the central North Pacific region, we can proceed to examine the vertical structure of the interdecadal temperature change. Figure 12a shows the temperature difference between 1978–89 and 1971–76 at 100-m depth, which lies within or near the base of the winter mixed layer; Fig. 12b shows the temperature difference between 1979–90 and 1972–77 at 250 m, a depth within the permanent thermocline except along the Kuroshio Extension where it lies near the base of the winter mixed layer; and Fig. 12c shows

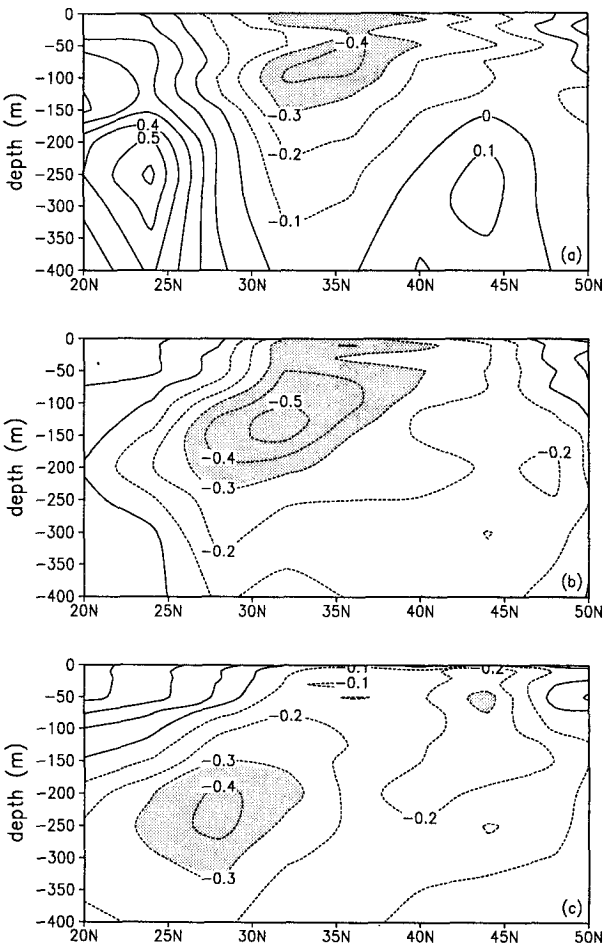

FIG. 10. Annual temperature anomalies as a function of depth and latitude for the longitude band 170°–145°W for (a) 1977–81, (b) 1982–86, and (c) 1987–91. Negative anomalies are dashed. Anomalies less than −0.3°C are shaded.

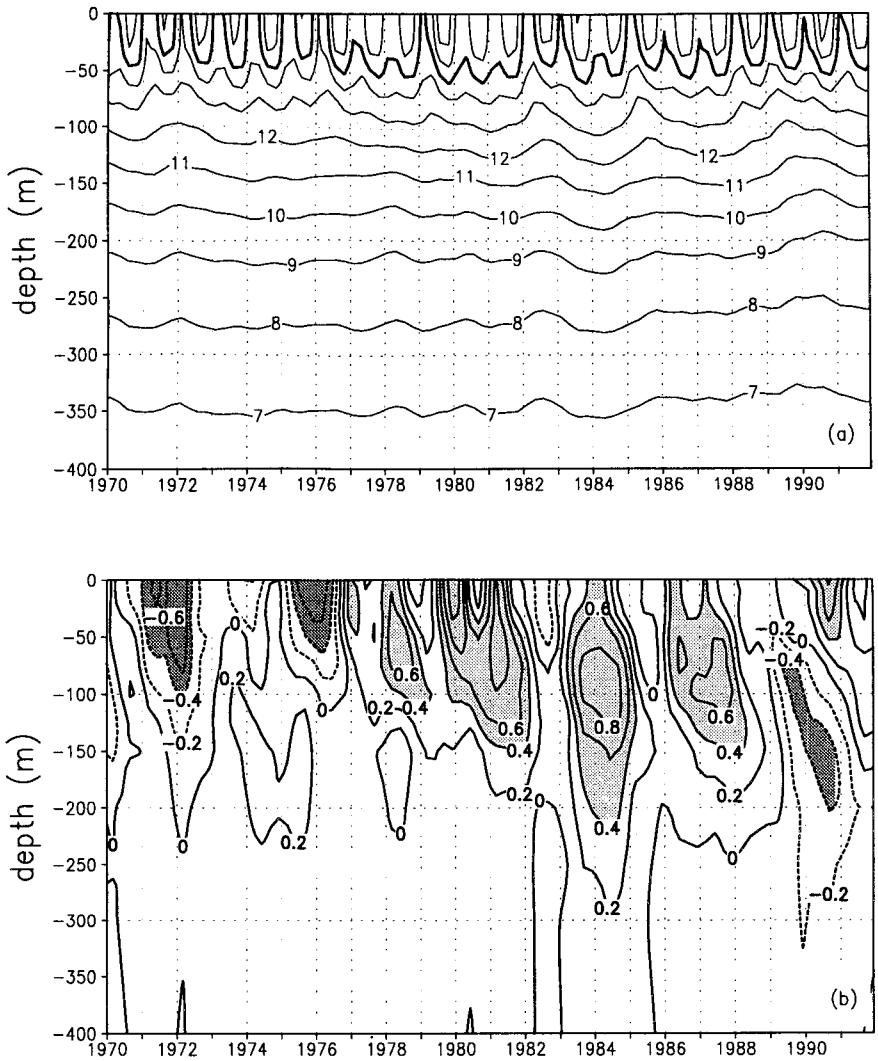

FIG. 11. Seasonal (a) total and (b) anomalous temperatures as in Fig. 7 but for the eastern North Pacific region.

the temperature difference between 1980–91 and 1972–78 at 400 m, which lies within the permanent thermocline. The years chosen to represent the interdecadal temperature change at the various depths were obtained from the time series of annual anomalies in the central Pacific region but may also be identified objectively on the basis of the leading EOF of annual temperature anomalies at the various depths (not shown; see also Levitus et al. 1994). The interdecadal difference at 100 m (Fig. 12a) is similar in pattern to that at the surface (Fig. 6b). The cooling in the central and western North Pacific is ~25% stronger at 100 m than at the surface due to the inclusion of weaker summer anomalies in the surface map. The warming in the eastern Pacific is about one-half as strong as at the surface. At 250 and 400 m (Figs. 12b and 12c), the largest interdecadal temperature differences (>0.5°C) occur along the Kuroshio Current Extension from the coast of Japan to ~170°W (e.g., along the axis of the largest mean meridional thermal gradient; recall Fig. 3). The anomalies in the western North Pacific at 400-m depth are shifted southward by several degrees of latitude with respect to those at the surface. The cooling in the central North Pacific, although smaller than that farther west, is statistically significant at the 95% level. There is negligible change in the eastern North Pacific at these depths.

Figure 13 shows a bar graph of seasonal temperature anomalies at selected depths along the Kuroshio Current Extension region [42°–34°N, 140°E–180°]. The rectangle in Fig. 12c marks the location of this region. Because this was an area of marginal data reliability (recall Fig. 6), SSTs from the COADS for the same region are shown in the top panel of Fig. 13. SST anom-

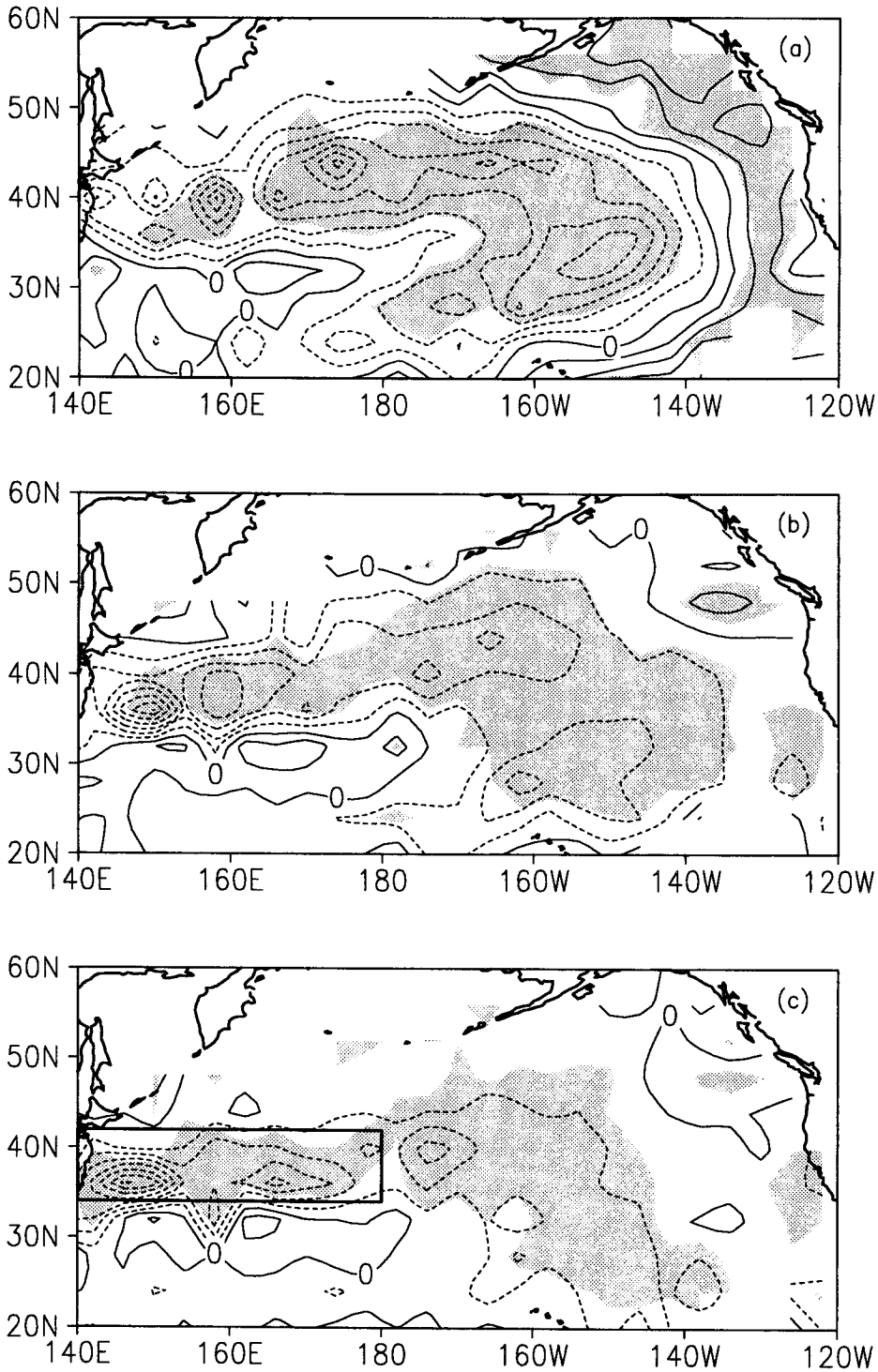

FIG. 12. Temperature difference between (a) 1978–89 and 1971–76 at 100 m, (b) 1979–90 and 1972–77 at 250 m and (c) 1980–91 and 1972–78 at 400 m. Contour interval is 0.25°C. Negative contours are dashed. Shading denotes SST differences that are significant at the 95% level. Rectangle in (c) shows location of the Kuroshio Current Extension region defined in the text.

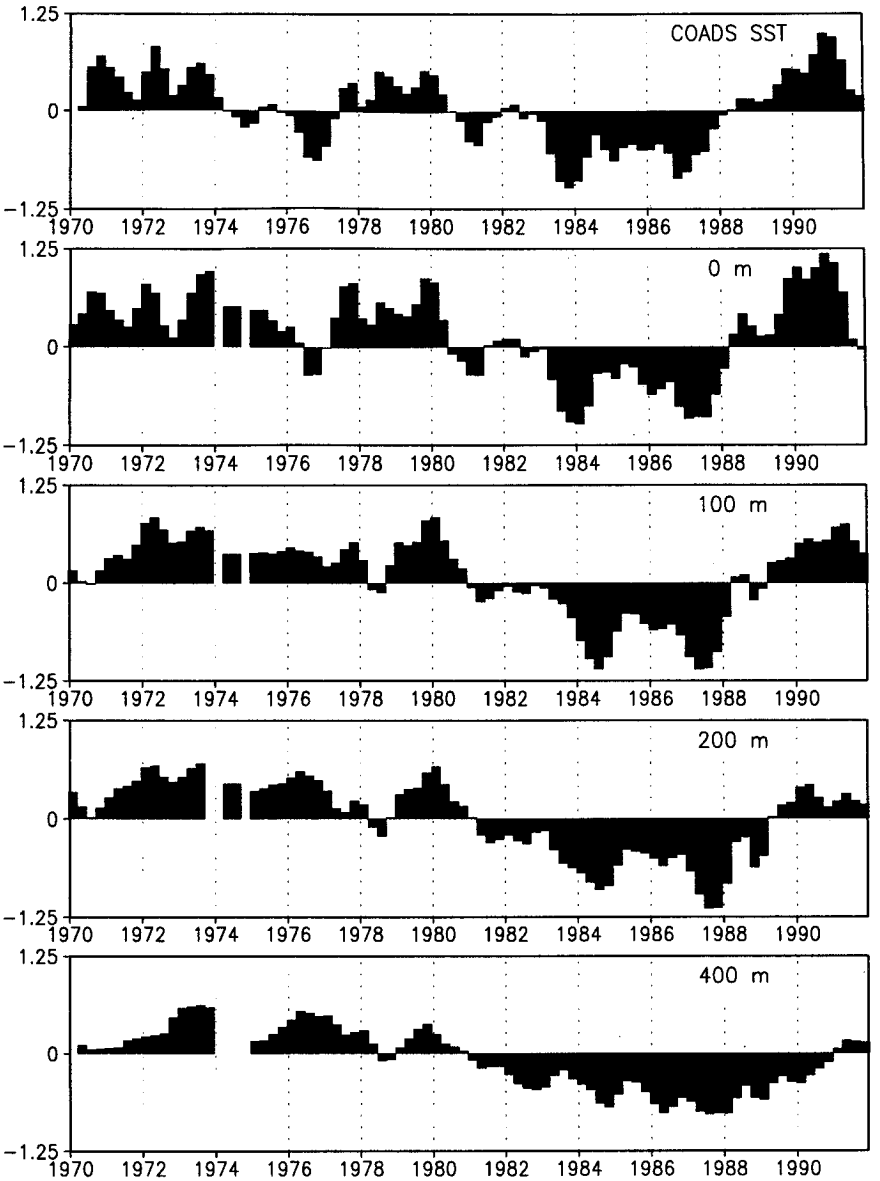

FIG. 13. Seasonal temperature anomalies (°C) in the Kuroshio Current Extension region at selected depths. Top panel shows SST anomalies from the COADS.

alies from the two datasets agree except during 1974 through early 1976, when the number of subsurface profiles was greatly reduced (note the missing values at depth). Unlike the central Pacific region, the thermal anomalies in the Kuroshio Extension region occur nearly simultaneously within the upper 400 m (with the exception of the warm anomaly near the end of the record) and show little attenuation with depth (note that the temperature scale is the same for all levels). We note that the transition to colder than normal temperatures in the Kuroshio Extension region occurs ~1981, several years after onset of cooling in the Central Pacific region.

d. Mixed layer depths

Next we examine whether the interdecadal variation in SST is accompanied by a change in MLD. Figure 14 shows the winter (Jan–Mar) MLD difference between 1977–88 and 1971–76. Positive (negative) MLD differences indicate a deepening (shoaling) of the mixed layer with time. Winter mixed layers deepened by more than 20 m over a large area of the central North Pacific and shoaled by more than 20 m in the Gulf of Alaska. Only a portion of the MLD changes in these areas exceeds the 95% significance level, reflecting in part the noisiness of the MLD data. A similar pattern of MLD

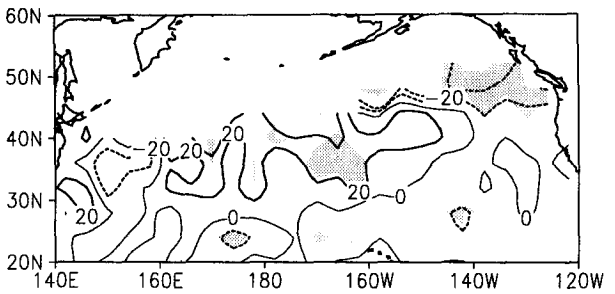

FIG. 14. Winter mixed layer depth (MLD) differences between 1977–88 and 1971–76. Contour interval is 20 m. Positive (negative) values denote deepening (shoaling) of the mixed layer with time. Shading denotes MLD differences that are significant at the 95% level.

change was obtained by Polovina et al. (1995) using a temperature gradient criterion for MLD.

Although the region of deeper mixed layers in the central North Pacific is roughly coincident with the area of lower SSTs (recall Fig. 6b), the largest changes in MLD occur over the northern half of the largest changes in SST (note that the interdecadal change of SST in winter is very similar to the annual mean). The interdecadal change in MLD over the eastern Pacific is near zero despite the large surface warming there. The lack of significant MLD changes in the eastern Pacific, and the northward shift of the deeper mixed layers relative to the coldest SST anomalies in the central Pacific, may be related to the mean vertical stratification beneath the mixed layer and the mean wind speed. In particular, we note that the mean vertical stratification at the base of the winter mixed layer increases, and the mean turbulent kinetic energy input by the wind decreases, to the south and east in the North Pacific [not shown, but see Figs. 7a and 11a and Oberhuber (1988) for a sense of the stratification and wind effects, respectively].

The pattern of interdecadal MLD changes in fall is similar to that in winter, although the magnitudes are less than half; no significant interdecadal MLD changes are found in spring and summer (not shown). We emphasize that only temperature variations contribute to the MLD changes shown in Fig. 14: Salinity variations may also play a role, particularly in the subpolar gyre north of ~42°N.

Figure 15 shows the time series of winter MLD and SST anomalies for the central Pacific region. Positive values denote deeper than normal mixed layers; note that the MLD curve is inverted. In general, above (below) normal SSTs correspond to shallower (deeper) than normal MLDs: the correlation coefficient between winter SST and MLD is −0.76. The largest MLD anomalies are on the order of 20–30 m, or 20%–30% of the long-term mean. The correlation coefficients between SST and MLD in the central Pacific region are −0.70 in fall, −0.48 in spring, and −0.42 in summer.

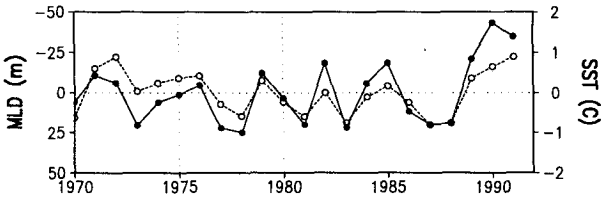

FIG. 15. Time series of winter mean MLD (solid curve) and SST (dashed curve) anomalies in the Central North Pacific Region. The MLD curve is inverted so that positive values correspond to deeper than normal mixed layers.

4. Discussion

The time–depth structure of the thermal anomalies in the central and eastern North Pacific regions strongly suggests that the atmosphere played a dominant role in forcing the interdecadal change in SST from 1970–76 to 1977–88, confirming the model results of Miller et al. (1994). (Note that this scenario does not preclude the possibility of positive feedback from the ocean to the atmosphere.) As shown by Miller et al., sensible and latent heat fluxes, horizontal advection by wind-driven Ekman currents, and buoyancy-driven vertical mixing all played a role in maintaining the interdecadal shift in SSTs.

The thermal changes were not confined to the mixed layer but penetrated into the upper portion of the permanent pycnocline in the subtropical gyre. In the central Pacific region, the temperature anomalies appeared to propagate downward to at least 400 m on both a rapid (~100 m yr^{-1}) and slow (~15 m yr^{-1}) timescale. In contrast, in the eastern Pacific region most of the variability was confined to above approximately 200–250 m. Can we understand the behavior of these thermal anomalies in light of dynamical processes op-

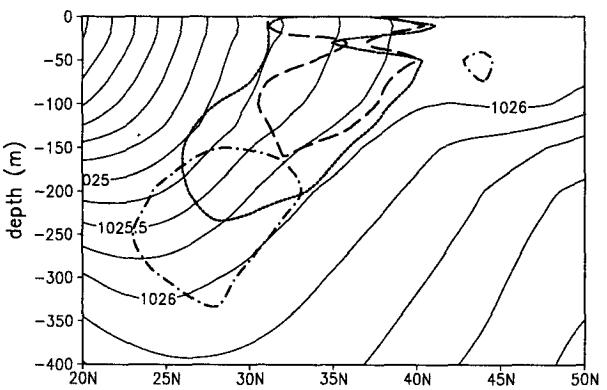

FIG. 16. The −0.3°C anomaly isotherms for 1977–81 (dashed line), 1982–86 (dotted line), and 1987–91 (dot–dashed line), superimposed upon the mean late-winter (February–April) isopycnals (kg m^{-3}; thin solid lines) as a function of depth and latitude for the longitude band 170°–145°W. The −0.3°C contours are taken from Fig. 10.

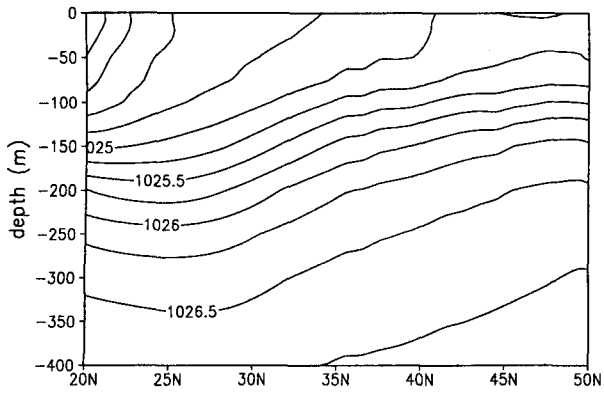

FIG. 17. Mean late-winter (Feb–Apr) isopycnals (kg m^{-3}) as a function of depth and latitude for the longitude band 134°–122°W.

erating within the permanent pycnocline? The ventilated thermocline theory provides a dynamical framework for interpreting some aspects of the behavior of the thermal anomalies in the central and eastern Pacific regions.

The concept of the permanent pycnocline as a layered system with flow along isopycnal surfaces was first introduced by Luyten et al. (1983) and developed further by Woods (1985), Bleck et al. (1989), Huang (1990), Marshall and Nurser (1992), and Liu and Pedlosky (1994), among others. In their model, ventilated layers are those where the isopycnals outcrop and become "exposed to air–sea interaction through mass exchange with the mixed layer" (Huang and Qiu 1994). The water subducted[1] from the mixed layer into the upper portion of the pycnocline in late winter conserves potential vorticity as it flows along isopycnal surfaces. Flow in these layers is controlled primarily by Ekman pumping resulting from wind stress curl, with the horizontal component obeying Sverdrup (1947) balance. Unventilated layers, shadow zones, are not in contact with the surface but may intersect east or west boundaries, or for deep layers be continuous, indicating recirculation gyres. Talley (1985), Huang and Qiu (1994), and Huang and Russell (1994) demonstrated the applicability of this model to the mean structure of the subtropical gyre in the North Pacific.

The upper 400 m of the central Pacific region resides in the ventilated portion of the subtropical gyre where the mean flow is southward and downward (Huang and Qiu 1994; Huang and Russell 1994). If the layered pycnocline model is valid and the observed temperature perturbations are small enough (or balanced by salinity variations in terms of their contribution to density) so as to not greatly alter the mean pycnocline structure, then the temperature anomalies formed in the deep mixed layer in winter should be subducted into the permanent pycnocline and flow southward and downward along surfaces of constant mean density. We examine this hypothesis in Fig. 16 by plotting the −0.3°C anomaly isotherms for three 5-yr periods spanning the duration of the interdecadal cooling (1977–81, 1982–86, and 1987–91; taken from Fig. 10), superimposed upon the mean late-winter isopycnals as a function of depth and latitude for the longitude band 170°–145°W. The initial anomalous cold water mass extends through the surface mixed layer where the density is nearly vertically uniform, spanning latitudes ~31°–40°N corresponding to a density range of 1025.25 ~ 1026 kg m^{-3}. The cold anomaly appears to be subducted into the permanent pycnocline at ~150-m depth and then moves downward and southward along the same density surfaces over the next two pentads. The rates of downward and southward movement, as estimated from the leading edge of the −0.3°C contours, are ~15 m yr^{-1} and ~0.25 cm s^{-1}, respectively, for the depth range 150–300 m. According to Huang and Qiu (1994), the mean downward Ekman pumping velocity in the region [36°–23°N, 170°–145°W] is approximately 25–40 m yr^{-1}. This yields a mean southward Sverdup flow of ~0.2–0.4 cm s^{-1} assuming a depth of 1–1.5 km for the wind-

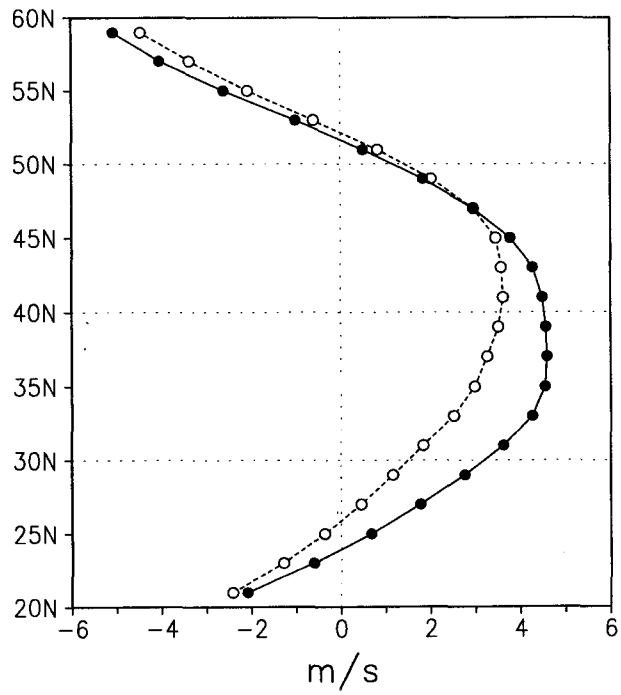

FIG. 18. Latitudinal profiles of winter mean (Nov–Mar) zonal winds (m s^{-1}) averaged across the Pacific for 1971–76 (dashed curve) and 1977–88 (solid curve). Positive (negative) values denote winds from the west (east).

[1] In addition to Ekman pumping, the subduction process includes a lateral induction component due to horizontal gradients of mixed layer depth; however, this component is small in the central and eastern North Pacific (Huang and Qiu 1994).

driven gyre (see Huang and Qiu 1994). Thus, the southward movement of the thermal anomalies is roughly consistent with the speed derived from the mean curl of the wind stress. There are few observations of vertical velocity in the upper portion of the subtropical gyre with which to compare the descent rate of the thermal anomalies. One such estimate by Hautala et al. (1994) for 24°N in the central Pacific yields a mean downward speed ~25 m yr^{-1} averaged over the upper 500 m, in line with the observed descent rate of the thermal anomalies.

As noted in section 3, the temperature anomalies in the eastern Pacific region are primarily confined to the upper 200–250 m. This result can also be interpreted in light of the ventilated thermocline theory. The results of Talley (1985), Huang and Qiu (1994), and Huang and Russell (1994) suggest that some of the isopycnal surfaces along the west coast of North America lie within the shadow zone and thus have no interaction with the surface mixed layer. As a result of the strong stratification even the ventilated layers tend to be horizontal and the mass transport within the layer is relatively small. Figure 17 shows the latitude–depth structure of the mean late-winter isopycnals in the longitude range 134°–122°W, along the west coast of North America. Isopycnal surfaces denser than ~1025.5 kg m^{-3} do not outcrop: Regions at or below this surface will not be ventilated. This isopycnal attains a maximum depth of ~200 m at 24°N. Thus, the lack of appreciable thermal variability below ~200–250 m in the eastern Pacific region is consistent with the notion of a shadow zone. Although desirable, tracing the southward/downward movement of the thermal anomalies in this region is problematic because the anomalies do not originate exclusively in the surface mixed layer (see Fig. 11b).

While the ventilated thermocline theory provides a dynamical context for the slow evolution of the interdecadal cooling in the central Pacific, the rates of descent of individual cold plumes (see Fig. 7b) are nearly an order of magnitude faster than that predicted by Ekman pumping. We note that similar rates of downward propagation (50–100 m per year) have been obtained by White and Walker (1974) for Ocean Weather Stations N (30°N, 140°W) and P (50°N, 145°W) and by White and Bernstein (1981) for the central midlatitude Pacific over a 1-year period. Further work is needed to understand the processes governing the vertical penetration of individual cold episodes. Plausible mechanisms include surface forcing and subsequent downward propagation of baroclinic Rossby waves, eddy mixing along isopycnals, and diapycnal mixing. We note that the downward group velocity of baroclinic Rossby waves in the subtropical gyre is on the order of 100 m yr^{-1} for reasonable choices of the parameters (see Gill 1982), although this value is very sensitive to the vertical wavelength.

In the foregoing discussion, we have emphasized the advective role of the *time-mean* flow within the ventilated thermocline. However, the wind-driven component of flow may not have been steady, as implied by the large-scale changes in surface wind stress across the North Pacific (Fig. 1). Figure 18 shows the winter mean (Nov–Mar) zonal wind profiles averaged across the Pacific basin for the periods 1971–76 and 1977–88. The profiles are based on 2° × 2° data from COADS and have been smoothed in latitude with a three-point binomial filter. The midlatitude westerlies intensified along their southern flank from 1971–76 to 1977–88, with the largest increases approaching 2 m s^{-1} or ~50% of the mean between 30° and 35°N. The intensification and southward shift of the mean westerlies across the Pacific would imply a change in the Sverdrup component of flow, a point also noted by Trenberth et al. (1990). In particular, the North Pacific subtropical gyre for which Sverdrup balance appears to hold (Hautala et al. 1994), may be in the process of adjusting to the altered wind field by strengthening and moving southward.

5. Summary

We used a newly available, extensive compilation of upper-ocean temperature profiles to study the vertical structure of thermal anomalies in the North Pacific during 1970–1991. A prominent decade-long perturbation in climate occured during this time period: surface waters cooled by ~1°C in the central and western North Pacific and warmed by about the same amount along the west coast of North America from late 1976 to 1988. Comparison with data from COADS suggests that the relatively sparse sampling of the subsurface data is adequate for describing the climate change.

The vertical structure of the thermal anomalies in the central North Pacific region shows a series of cold pulses, beginning in the fall of 1976 and continuing until late 1988, that appear to originate at the surface and descend with time into the main thermocline. Individual cold events descend rapidly (~100 m yr^{-1}), superimposed upon a slower cooling (~15 m yr^{-1}). The interdecadal climate change, while evident at the surface, is most prominent below ~150 m where interannual variations are small. Unlike the central Pacific region, the temperature changes along the west coast of North America appear to be confined to approximately the upper 200–250 m. The structure of the interdecadal thermal variations in the eastern and central Pacific appears to be consistent with the dynamics of the ventilated thermocline.

Changes in MLD were found to accompany the thermal anomalies, but their spatial distribution was not identical to the pattern of SST change. In particular, the decade-long cool period in the central North Pacific was accompanied by a ~20 m deepening of the mixed layer in winter, but no significant changes in MLD were

found along the west coast of North America. It is suggested that other factors such as the stratification beneath the mixed layer and synoptic wind forcing may play a role in determining the distribution of MLD anomalies.

Decadal-scale thermal changes along the Kuroshio Current Extension Region were prominent at depths below ~200 m. Further study of the dynamical role of the western boundary current in producing these thermal changes, as well as its links to the tropical Pacific (cf. Qiu and Joyce 1992), is needed to better understand the causes of the Pacific climate change.

Acknowledgments. We thank S. Levitus, T. Boyer, and M. Conkright for providing the upper-ocean temperature profiles. We also thank the anonymous reviewers, W. Large, and Z. Liu for their comments, which helped to clarify our interpretation of the results. S. Peng and D. S. Battisti provided valuable suggestions on an earlier draft. This work was supported by a grant from the NOAA Office of Global Programs.

REFERENCES

Antonov, J. I., 1993: Linear trends of temperature at intermediate and deep layers of the North Atlantic and North Pacific Oceans: 1957–1981. *J. Climate,* **6,** 1928–1942.

Beamish, R. J., and D. R. Bouillon, 1993: Pacific salmon production trends in relation to climate. *Can. J. Fish. Aquat. Sci.,* **50,** 1002–1016.

Bleck, R., H. P. Hanson, D. Hu, and E. B. Kraus, 1989: Mixed layer-thermocline interaction in a three-dimensional isopycnic coordinate model. *J. Phys. Oceanogr.,* **19,** 1417–1439.

Boyer, T., and S. Levitus, 1994: Quality control and processing of historical oceanographic temperature, salinity and oxygen data. NOAA Tech. Rep. NESDIS 81, 64 pp. [National Oceanic and Atmospheric Administration, U.S. Govt. Printing Office, Washington, DC]

Cayan, D. R., A. J. Miller, T. P. Barnett, N. E. Graham, J. N. Ritchie, and J. M. Oberhuber, 1995: Seasonal–interannual fluctuations in surface temperature over the Pacific: Effects of monthly winds and heat fluxes. *Climate Variability on Decade to Century Time Scales.* National Academy of Sciences Press, 612 pp.

Chen, T. C., H. van Loon, K. D. Wu, and M. C. Yen, 1992: Changes in the atmospheric circulation over the North Pacific–North America area since 1950. *J. Meteor. Soc. Japan,* **70,** 1137–1146.

Douglas, A. V., D. R. Cayan, and J. Namias, 1982: Large-scale changes in North Pacific and North American weather patterns in recent decades. *Mon. Wea. Rev.,* **110,** 1851–1862.

Ebbesmeyer, C. C., D. R. Cayan, D. R. McClain, F. H. Nichols, D. H. Peterson, and K. T. Redmond, 1991: 1976 step in the Pacific climate: Forty environmental changes between 1968–1975 and 1977–1984. *Proc. Seventh Annual Pacific Climate Workshop (PACLIM),* Asilomar, CA, California Department of Water Resources, 115–126.

Enfield, D. B., and J. S. Allen, 1980: On the structure and dynamics of monthly sea level anomalies along the Pacific coast of North and South America. *J. Phys. Oceanogr.,* **10,** 557–588.

Gill, A. E., 1982: *Atmosphere–Ocean Dynamics.* Academic Press, 662 pp.

Graham, N. E., 1994: Decadal-scale climate variability in the tropical and North Pacific during the 1970s and 1980s: Observations and model results. *Climate Dyn.,* **6,** 135–162.

——, T. P. Barnett, R. Wilde, M. Ponater, and S. Schubert, 1994: On the roles of tropical and midlatitude SSTs in forcing interannual to interdecadal variability in the winter Northern Hemisphere circulation. *J. Climate,* **7,** 1416–1442.

Hautala, S. L., D. H. Roemmich, and W. J. Schmitz, 1994: Is the North Pacific in Sverdrup balance along 24°N? *J. Geophys. Res.,* **99,** 16 041–16052.

Huang, R. X., 1990: On the three-dimensional structure of the wind-driven circulation in the North Atlantic. *Dyn. Atmos. Oceans,* **15,** 117–159.

——, and B. Qiu, 1994: Three-dimensional structure of the wind-driven circulation in the subtropical North Pacific. *J. Phys. Oceanogr.,* **24,** 1608–1622.

——, and S. Russell, 1994: Ventilation of the subtropical North Pacific. *J. Phys. Oceanogr.,* **24,** 2589–2604.

Kumar, A., A. Leetmaa, and M. Ji, 1994: Simulations of atmospheric variability induced by sea surface temperatures and implications for global warming. *Science,* **266,** 632–634.

Latif, M., and T. P. Barnett, 1994: Causes of decadal climate variability over the North Pacific and North America. *Science,* **266,** 634–637.

Levitus, S., 1982: *Climatological Atlas of the World Ocean.* NOAA Prof. Paper No. 13, U.S. Govt. Printing Office, Washington, D.C., 178 pp.

——, and T. P. Boyer, 1994: *NOAA Atlas NESDIS 4; World Ocean Atlas 1994.* Vol. 4, *Temperature.* U.S. Govt. Printing Office, 117 pp.

——, ——, and J. Antonov, 1994: *NOAA Atlas NESDIS 5; World Ocean Atlas 1994.* Vol. 5, *Interannual Variability of Upper Ocean Thermal Structure.* U.S. Govt. Printing Office. 176 pp.

Liu, Z., and J. Pedlosky, 1994: Thermocline forced by annual and decadal surface temperature variation. *J. Phys. Oceanogr.,* **24,** 587–608.

Luyten, J. R., J. Pedlosky, and H. Stommel, 1983: The ventilated thermocline. *J. Phys. Oceanogr.,* **13,** 292–309.

Marshall, J. C., and A. J. G. Nurser, 1992: Fluid dynamics of thermocline ventilation. *J. Phys. Oceanogr.,* **22,** 583–595.

Miller, A. J., D. R. Cayan, T. P. Barnett, N. E. Graham, and J. M. Oberhuber, 1994: Interdecadal variability of the Pacific Ocean: Model response to observed heat flux and wind stress anomalies. *Climate Dyn.,* **10,** 287–302.

Namias, J., X. Yuan, and D. R. Cayan, 1988: Persistence of North Pacific sea surface temperature and atmospheric flow patterns. *J. Climate,* **1,** 682–703.

Nitta, T., and S. Yamada, 1989: Recent warming of tropical sea surface temperature and its relationship to the Northern Hemisphere circulation. *J. Meteor. Soc. Japan,* **67,** 375–383.

Oberhuber, J. M., 1988: An atlas based on the COADS data set: The budgets of heat, buoyancy and turbulent kinetic energy at the surface of the global ocean. Max-Planck-Institute for Meteorology Rep. 15, Hamburg, Germany. 20 pp. plus 19 figures.

Pares-Sierra, A., and J. J. O'Brien, 1989: The seasonal and interannual variability of the California Current system: A numerical model. *J. Geophys. Res.,* **94,** 3159–3180.

Polovina, J. J., G. T. Mitchum, and G. T. Evans, 1995: Decadal and basin-scale variation in mixed layer depth and the impact on biological production in the Central and North Pacific, 1960–88. *Deep-Sea Res.,* **42,** 1701–1716.

Qiu, B., and T. M. Joyce, 1992: Interannual variability in the mid- and low-latitude western North Pacific. *J. Phys. Oceanogr.,* **22,** 1062–1079.

Rienecker, M. M., and C. N. K. Mooers, 1986: The 1982–1983 El Niño signal off Northern California. *J. Geophys. Res.,* **91,** 6597–6608.

Simpson, J. J., 1983: Large scale thermal anomalies in the California current during the 1982–83 El Niño. *Geophys. Res. Lett.,* **10,** 937–940.

Suga, T., and K. Hanawa, 1990: The mixed-layer climatology in the northwestern part of the North Pacific subtropical gyre and the formation area of subtropical mode water. *J. Mar. Res.,* **48,** 543–566.

Sverdrup, H. U., 1947: Wind-driven currents in a baroclinic ocean, with application to the equatorial currents of the eastern Pacific. *Proc. Natl. Acad. Sci. U.S.A.*, **33,** 318–326.

Talley, L. D., 1985: Ventilation of the subtropical North Pacific: The shallow salinity minimum. *J. Phys. Oceanogr.,* **15,** 633–649.

——, and W. B. White, 1987: Estimates of time and space scales at 300 m in the midlatitude North Pacific from the TRANSPAC XBT Program. *J. Phys. Oceanogr.,* **17,** 2168–2188.

Timlin, M., C. Deser, and M. Alexander, 1995: Upper ocean thermal changes in the North Pacific during 1970–1992. *19th Ann. Climate Diagnostic Workshop,* U.S. Dept. of Commerce, NOAA, NWS, and Climate Prediction Center, College Park, MD, 338–341.

Trenberth, K. E., 1990: Recent observed interdecadal climate changes in the Northern Hemisphere. *Bull. Amer. Meteor. Soc.,* **71,** 988–993.

——, and J. W. Hurrell, 1994: Decadal atmosphere–ocean variations in the Pacific. *Climate Dyn.,* **9,** 303–319.

——, W. G. Large, and J. G. Olson, 1990: The mean annual cycle in global ocean wind stress. *J. Phys. Oceanogr.,* **20,** 1742–1760.

Venrick, E. L., J. A. McGowan, D. R. Cayan, and T. L. Hayward, 1987: Climate and chlorophyll a: Long-term trends in the central North Pacific Ocean. *Science,* **238,** 70–72.

Weare, B. C., A. R. Navato, and R. E. Newell, 1976: Empirical orthogonal function analysis of Pacific Ocean sea surface temperatures. *J. Phys. Oceanogr.,* **6,** 671–678.

White, W. B., and A. E. Walker, 1974: Time and depth of anomalous subsurface temperature at Ocean Weather Stations P, N, and V in the North Pacific. *J. Geophys. Res.,* **79,** 4517–4522.

——, and R. Bernstein, 1981: Large-scale vertical eddy diffusion in the main pycnocline of the central North Pacific. *J. Phys. Oceanogr.,* **11,** 434–441.

Woods, J. D., 1985: The physics of thermocline ventilation. *Coupled Ocean–Atmosphere Models.* Chapter 34. J. C. J. Nihoul, Ed., Elsevier, 543–590.

Yan, X.-H., and A. Okubo, 1992: Three-dimensional analytical model for the mixed layer depth. *J. Geophys. Res.,* **97,** 20 201–20 226.